J. Plasma Physics (2006), *vol.* 72, *part* 1, *pp.* 85–103. © 2005 Cambridge University Press
doi:10.1017/S002237780500382X first published online 25 Nov. 2005 Printed in the United Kingdom

Dynamical conductivity of the Lorentz–Vlasov plasma model

B. U. FELDERHOF[1] and THIN VEHNS[2]

[1]Institut für Theoretische Physik A, RWTH Aachen, Templergraben 55, 52056 Aachen, Germany
(ufelder@physik.rwth-aachen.de)

[2]SAP AG, Neurottstrasse 16, 69190 Walldorf, Germany

(Received 13 September 2004 and accepted 20 October 2004)

Abstract. In the Lorentz–Vlasov model of a plasma the ions are assumed to be fixed in space with disordered distribution, and the Coulomb interaction between electrons is approximated by the Vlasov field, calculated self-consistently from the electron position–momentum distribution function. If correlations between ions are neglected, then the dynamical conductivity of the plasma may be evaluated from the dynamics of the electron gas in interaction with a single ion, the remaining ions being approximated by a uniform background. In dielectric or energy-loss theory, the dynamical friction coefficient is expressed in terms of the dielectric function of the uniform electron gas. A more detailed theory must take full account of the scattering of electrons by the selected ion. It is shown for an electron gas at zero temperature and metallic density, and for a simple ion pseudopotential, that the frequency dependence of the friction coefficient differs appreciably from that predicted by energy-loss theory.

1. Introduction

The theory of electrical conductivity of plasmas has a long and distinguished history. The conductivity is dominated by the motion of electrons colliding with the ions, which in good approximation may be assumed to remain static. An elementary calculation of the electron–ion collision frequency shows that binary collisions lead to a divergent cross section due to the long range of the Coulomb interaction. Thus, collective effects must be taken into account. In the simplest fashion this is accomplished by a cutoff of the Coulomb interaction at the Debye screening length. This leads to a finite collision frequency proportional to a Coulomb logarithm [1]. A more sophisticated calculation accounts for the dynamics of the electron gas. In dielectric or energy-loss theory the collision frequency, or equivalently the dynamical friction coefficient or photoabsorption cross section, is expressed in terms of the dielectric function of the uniform electron gas [2, 3]. This implies a simplified description of the scattering of electrons by the selected ion. A more detailed theory must take full account of the electron–ion interaction.

In the following we first discuss the derivation of the theoretical expression for the dynamical friction coefficient in the framework of a classical model with neglect of ion correlations. The derivation is based on linear response theory and a cluster expansion of the average over the probability distribution of ion configurations.

https://doi.org/10.1017/S002237780500382X Published online by Cambridge University Press

In the lowest order of the cluster expansion this leads to the single-ion friction coefficient. The derivation is presented in Secs 2 and 3, and may be skipped at first reading. The expression for the friction coefficient is discussed in Sec. 4. The approximate expression of energy-loss theory is studied in Sec. 5, with a slight improvement based on complete static screening of the ion. By way of an example, the approximate expressions for the dynamical friction coefficient are evaluated in Sec. 6 for the particular case of a cold electron gas at metallic density, i.e. in the framework of Thomas–Fermi theory. The classical calculation leads to divergence difficulties associated with the point-like nature of the ion. In order to avoid these, we use a simple ion pseudopotential, constructed on the basis of an exact quantummechanical identity. The complete classical calculation of the dynamical friction coefficient with full account of the ion pseudopotential is discussed in Sec. 7. Numerical results for the model of Sec. 6 are presented in Sec. 8, and compared with the result of energy-loss theory. The complete calculation leads to appreciable deviation from the prediction of energy-loss theory.

2. Lorentz–Vlasov model

We consider a classical plasma consisting of electrons of charge $-e$, mass m, interacting with identical spherically symmetric ions. The whole system is electrically neutral and approximately uniform. Since the ions are much heavier than the electrons, their motion will be neglected. The ions act as fixed scatterers for the electrons. The electrons interact by Coulomb interaction, approximated by a self-consistent Vlasov field. The electron gas is perturbed by an applied, uniform, time-dependent electric field $\mathbf{E}(t)$.

For mathematical convenience periodic boundary conditions are imposed, with a simple cubic lattice dividing space into unit cells of volume Ω. Each cell contains N electrons and N_i ions of charge $Z\mathrm{e}$. Electroneutrality implies $N = ZN_\mathrm{i}$. In Vlasov approximation the dynamics of the electrons in a unit cell are described by the single electron Hamiltonian

$$H(\mathbf{r},\mathbf{p},t) = \frac{p^2}{2m} + \Phi(\mathbf{r}) - e\phi(\mathbf{r},t) + e\mathbf{E}(t)\cdot\mathbf{r} \tag{2.1}$$

with ion potential

$$\Phi(\mathbf{r}) = \sum_{j=1}^{N_\mathrm{i}} v(\mathbf{r}-\mathbf{R}_j) \tag{2.2}$$

and electrostatic potential

$$\phi(\mathbf{r},t) = -e\int_\Omega \int w(\mathbf{r}-\mathbf{r}')f(\mathbf{r}',\mathbf{p}',t)\,d\mathbf{r}'\,d\mathbf{p}'. \tag{2.3}$$

Here $w(\mathbf{r})$ is the Wigner potential, i.e. the solution of Poisson's equation for a simple cubic lattice of unit point charges with neutralizing background [4]. The electron distribution in phase space $f(\mathbf{r},\mathbf{p},t)$ is required to be periodic in $\mathbf{r}$. It is normalized to

$$\int_\Omega \int f(\mathbf{r},\mathbf{p},t)\,d\mathbf{r}\,d\mathbf{p} = N. \tag{2.4}$$

Since the ions are charged the ion potential $v(\mathbf{r}-\mathbf{R}_j)$ contains a long-range part $-Z\mathrm{e}^2 w(\mathbf{r}-\mathbf{R}_j)$. The potential is due to the Coulomb potential of the nucleus,

https://doi.org/10.1017/S002237780500382X Published online by Cambridge University Press

bound electrons, and the corresponding neutralizing background. The short distance behaviour of the potential $v(\mathbf{r})$ must be determined by quantummechanical considerations. The time evolution of the distribution of mobile electrons is given by

$$\frac{\partial f}{\partial t} + \frac{\mathbf{p}}{m} \cdot \frac{\partial f}{\partial \mathbf{r}} + \mathscr{F} \cdot \frac{\partial f}{\partial \mathbf{p}} = e\mathbf{E}(t) \cdot \frac{\partial f}{\partial \mathbf{p}}, \tag{2.5}$$

where $\mathscr{F}(\mathbf{r}, t)$ is the force exerted by ions and electrons

$$\mathscr{F}(\mathbf{r}, t) = -\frac{\partial \Phi}{\partial \mathbf{r}} + e\frac{\partial \phi}{\partial \mathbf{r}}. \tag{2.6}$$

For a vanishing applied field, (2.5) has stationary solutions of the form $f_0(H_0)$ with time-independent Hamiltonian

$$H_0(\mathbf{r}, \mathbf{p}) = \frac{p^2}{2m} + \Phi(\mathbf{r}) - e\phi_0(\mathbf{r}) \tag{2.7}$$

with $\phi_0(\mathbf{r})$ calculated from the distribution $f_0(H_0)$ via (2.3). In linear response theory the distribution function is expanded in the applied field as

$$f(\mathbf{r}, \mathbf{p}, t) = f_0(H_0) + f_1(\mathbf{r}, \mathbf{p}, t) + o(E), \tag{2.8}$$

where $f_1(\mathbf{r}, \mathbf{p}, t)$ is linear in $\mathbf{E}$. It satisfies the equation

$$\frac{\partial f_1}{\partial t} + \mathscr{L} f_1 = e\mathbf{E} \cdot \frac{\partial f_0}{\partial \mathbf{p}} \tag{2.9}$$

with the linear evolution operator $\mathscr{L}$ given by

$$\mathscr{L} = \mathscr{L}_0 + \mathscr{V}, \tag{2.10}$$

where $\mathscr{L}_0$ is the single electron Liouville operator corresponding to H_0

$$\mathscr{L}_0 A = \{A, H_0\} = \frac{\mathbf{p}}{m} \cdot \frac{\partial A}{\partial \mathbf{r}} + \mathscr{F}_0 \cdot \frac{\partial A}{\partial \mathbf{p}}, \tag{2.11}$$

and the linear operator $\mathscr{V}$ is defined by

$$\mathscr{V} A = -e^2 f_0' \frac{\mathbf{p}}{m} \cdot \frac{\partial}{\partial \mathbf{r}} \int_\Omega \int w(\mathbf{r} - \mathbf{r}') A(\mathbf{r}', \mathbf{p}')\, d\mathbf{r}'\, d\mathbf{p}', \tag{2.12}$$

where $f_0' = df_0/dH_0$. For harmonic oscillating field $\mathbf{E}(t) = \mathbf{E}_0 \exp(-i\omega t)$ we consider the solution of (2.9) oscillating with the same time factor $f_1(\mathbf{r}, \mathbf{p}, t) = f_1(\mathbf{r}, \mathbf{p}) \exp(-i\omega t)$ with $f_1(\mathbf{r}, \mathbf{p})$ satisfying

$$(-i\omega + \mathscr{L}) f_1 = \frac{e}{m} \mathbf{E}_0 \cdot \mathbf{p} f_0'. \tag{2.13}$$

The formal solution is

$$f_1 = \frac{e}{m} (-i\omega + \mathscr{L})^{-1} \mathbf{E}_0 \cdot \mathbf{p} f_0'. \tag{2.14}$$

We are interested in the mean electron velocity $\mathbf{V}(t)$. In the stationary state $\mathbf{V}_0 = 0$, by symmetry in the momentum. To first order in $\mathbf{E}_0$, with omission of the exponential time factor,

$$\mathbf{V}_1 = \frac{1}{N} \int_\Omega \int \frac{\mathbf{p}}{m} f_1(\mathbf{r}, \mathbf{p})\, d\mathbf{r}\, d\mathbf{p}. \tag{2.15}$$

Substituting from (2.14) we find that the first-order mean velocity is given by

$$\mathbf{V}_1 = -e\mathscr{Y} \cdot \mathbf{E}_0 \tag{2.16}$$

https://doi.org/10.1017/S002237780500382X Published online by Cambridge University Press

with admittance tensor

$$\mathscr{Y}(\omega, \mathbf{X}, \Omega) = \frac{-1}{Nm^2} \int_\Omega \int \mathbf{p}(-i\omega + \mathscr{L})^{-1} \mathbf{p} f_0' \, d\mathbf{r} \, d\mathbf{p}. \tag{2.17}$$

The tensor depends parametrically on the configuration $\mathbf{X} = (\mathbf{R}_1, \ldots, \mathbf{R}_N)$ of ions in the unit cell. Below we perform an average over the probability distribution of configurations, which is assumed known.

3. Friction tensor

In the case of independent electrons the admittance can be re-expressed in terms of a friction tensor that can be evaluated from two time-correlation functions [5–7]. Similar relations can be derived in the presence of Coulomb interactions treated in Vlasov approximation.

We consider the product $\mathbf{p} f_0'$ appearing on the right-hand side of (2.13), and write it in the form

$$\mathbf{p} f_0' = \mathscr{G}(-i\omega + \mathscr{L}) \mathbf{p} f_0', \tag{3.1}$$

where $\mathscr{G}$ is the inverse operator $\mathscr{G}(\omega) = (-i\omega + \mathscr{L})^{-1}$. From (2.12) we find $\mathscr{V} \mathbf{p} f_0' = 0$, since f_0' is even in $\mathbf{p}$. Hence, $\mathbf{p} f_0'$ can be expressed as the sum

$$\mathbf{p} f_0' = -i\omega \mathscr{G} \mathbf{p} f_0' + \mathscr{G} \mathscr{F}_0 f_0', \tag{3.2}$$

where

$$\mathscr{F}_0(\mathbf{r}) = -\frac{\partial \Phi}{\partial \mathbf{r}} + e \frac{\partial \phi_0}{\partial \mathbf{r}} \tag{3.3}$$

is the total force corresponding to the stationary distribution f_0. Multiplying (3.2) by the bare scattering force $\mathscr{F}_\mathrm{b} = -\partial \Phi / \partial \mathbf{r}$ and integrating over phase space, we therefore find the identity

$$-i\omega \int_\Omega \int \mathscr{F}_\mathrm{b} \mathscr{G} \mathbf{p} f_0' \, d\mathbf{r} \, d\mathbf{p} + \int_\Omega \int \mathscr{F}_b \mathscr{G} \mathscr{F}_0 f_0' \, d\mathbf{r} \, d\mathbf{p} = 0. \tag{3.4}$$

We write this in the form

$$-i\omega m \mathbf{A}_\mathrm{Fv}(\omega, \mathbf{X}, \Omega) + \boldsymbol{\zeta}_\mathrm{t}(\omega, \mathbf{X}, \Omega) = 0 \tag{3.5}$$

with the tensors $\mathbf{A}_\mathrm{Fv}$ and $\boldsymbol{\zeta}_\mathrm{t}$ defined by

$$\begin{aligned} \mathbf{A}_\mathrm{Fv}(\omega, \mathbf{X}, \Omega) &= \frac{-1}{Nm} \int_\Omega \int \mathscr{F}_\mathrm{b} \mathscr{G} \mathbf{p} f_0' \, d\mathbf{r} \, d\mathbf{p}, \\ \boldsymbol{\zeta}_\mathrm{t}(\omega, \mathbf{X}, \Omega) &= \frac{-1}{N} \int_\Omega \int \mathscr{F}_\mathrm{b} \mathscr{G} \mathscr{F}_0 f_0' \, d\mathbf{r} \, d\mathbf{p}. \end{aligned} \tag{3.6}$$

The tensor $\mathbf{A}_\mathrm{Fv}$ can be related directly to the admittance tensor $\mathscr{Y}$, defined in (2.17). Explicitly (2.13) reads

$$-i\omega f_1 + \frac{\mathbf{p}}{m} \cdot \frac{\partial f_1}{\partial \mathbf{r}} + \mathscr{F}_0 \cdot \frac{\partial f_1}{\partial \mathbf{p}} + \mathscr{V} f_1 = e \mathbf{E}_0 \cdot \frac{\partial f_0}{\partial \mathbf{p}}. \tag{3.7}$$

Multiplying this by $\mathbf{p}/Nm$, using the definition (2.15), and integrating by parts on the right-hand side we find

$$-i\omega \mathbf{V}_1 + \frac{1}{Nm^2} \int_\Omega \int \mathbf{p}\mathbf{p} \cdot \frac{\partial f_1}{\partial \mathbf{r}} \, d\mathbf{r} \, d\mathbf{p} + \frac{1}{Nm} \int_\Omega \int \mathbf{p} \mathscr{F}_\mathrm{b} \cdot \frac{\partial f_1}{\partial \mathbf{p}} \, d\mathbf{r} \, d\mathbf{p} = -\frac{e}{m} \mathbf{E}_0. \tag{3.8}$$

https://doi.org/10.1017/S002237780500382X Published online by Cambridge University Press

Here we have used

$$e\int_\Omega\int \mathbf{p}\frac{\partial\phi_0}{\partial\mathbf{r}}\cdot\frac{\partial f_1}{\partial\mathbf{p}}\,d\mathbf{r}\,d\mathbf{p}+\int_\Omega\int \mathbf{p}\mathscr{V}f_1\,d\mathbf{r}\,d\mathbf{p}=0 \tag{3.9}$$

for arbitrary $f_1(\mathbf{r},\mathbf{p})$. This identity follows easily by partial integration in $\mathbf{p}$ and use of (2.3) and (2.12). The second term on the left-hand side of (3.8) vanishes by periodicity, and in the third we can integrate by parts. This yields

$$-i\omega\mathbf{V}_1-\frac{1}{Nm}\int_\Omega\int \mathscr{F}_{\mathrm{b}}f_1\,d\mathbf{r}\,d\mathbf{p}=-\frac{e}{m}\mathbf{E}_0. \tag{3.10}$$

Substituting the solution f_1 from (2.14) and using the definition (2.16) we therefore find

$$\mathscr{Y}(\omega,\mathbf{X},\Omega)=\frac{-1}{i\omega m}[\mathbf{1}+\mathbf{A}_{\mathrm{Fv}}(\omega,\mathbf{X},\Omega)]. \tag{3.11}$$

With the friction tensor $\boldsymbol{\zeta}(\omega,\mathbf{X},\Omega)$ defined by

$$\mathscr{Y}(\omega,\mathbf{X},\Omega)=[-i\omega m\mathbf{1}+\boldsymbol{\zeta}(\omega,\mathbf{X},\Omega)]^{-1} \tag{3.12}$$

we therefore have, as for independent electrons [7],

$$\boldsymbol{\zeta}(\omega,\mathbf{X},\Omega)=\boldsymbol{\zeta}_{\mathrm{t}}(\omega,\mathbf{X},\Omega)[\mathbf{1}+\mathbf{A}_{\mathrm{Fv}}(\omega,\mathbf{X},\Omega)]^{-1} \tag{3.13}$$

with the definitions (3.6) of the tensors $\mathbf{A}_{\mathrm{Fv}}$ and $\boldsymbol{\zeta}_{\mathrm{t}}$.

4. Single-ion friction coefficient

For a disordered system of ions we can average the exact relations derived above over the probability distribution of configurations $P(\mathbf{X})$, assumed given. The system is assumed to become uniform and isotropic in the thermodynamic limit. Then, by the same arguments as for a system of independent electrons [7], we arrive for a low density of ions at the expression for the friction coefficient

$$\zeta_1(\omega)=-\frac{1}{3}n_{\mathrm{i}}\iint \mathbf{F}_{\mathrm{b}}(\mathbf{r})\cdot G(1)\mathbf{F}_0(\mathbf{r})\varphi_0'(\varepsilon)\,d\mathbf{r}\,d\mathbf{p}, \tag{4.1}$$

where n_{i} is the density of ions, and $\varphi_0'(\varepsilon)$ is the derivative with respect to energy ε of the stationary electron distribution $\varphi_0(\varepsilon)$, normalized such that

$$\int \varphi_0(H_0(1))\,d\mathbf{p}\to 1\quad\text{as } r\to\infty. \tag{4.2}$$

Here ε is the value of the Hamiltonian

$$H_0(\mathbf{r},\mathbf{p};1)=\frac{p^2}{2m}+v_0(r),\quad v_0(r)=v_{\mathrm{b}}(r)-e\phi_0(r) \tag{4.3}$$

for an electron with a single ion centred at the origin. The bare ion potential $v_{\mathrm{b}}(r)$ is centrally symmetric and has long-range part $-Ze^2/r$. It is screened by the potential $-e\phi_0(r)$. The bare force $\mathbf{F}_{\mathrm{b}}(\mathbf{r})$ in (4.1) is simply the gradient $-\partial v_{\mathrm{b}}/\partial\mathbf{r}$, and the operator $G(1)$ is the inverse $(-i\omega+\mathscr{L}(1))^{-1}$ with evolution operator $\mathscr{L}(1)$ for the linearized Vlasov equation corresponding to the equilibrium distribution

$$f_0(r,p)=n_0^{(0)}\varphi_0(H_0(1)), \tag{4.4}$$

https://doi.org/10.1017/S002237780500382X Published online by Cambridge University Press

where $n_0^{(0)}$ is the asymptotic free-electron density. The potential $\phi_0(r)$ must be found self-consistently from the solution of Poisson's equation

$$\nabla^2\phi_0 = 4\pi e\left[\int f_0(r,p)\,d\mathbf{p} - n_0^{(0)}\right]. \tag{4.5}$$

In practical applications the distribution $f_0(r,p)$ will be a Maxwell–Boltzmann or Fermi–Dirac distribution. The force $\mathbf{F}_0(\mathbf{r})$ in (4.1) is given by

$$\mathbf{F}_0(\mathbf{r}) = -\frac{\partial v_0}{\partial \mathbf{r}} = \mathbf{F}_\mathrm{b}(\mathbf{r}) + e\frac{\partial \phi_0}{\partial \mathbf{r}}. \tag{4.6}$$

Some bound electrons are included quantummechanically, and make themselves felt in the bare ion potential $v_\mathrm{b}(r)$. Mobile electrons with negative energy ε are bound classically. The bare ion charge Ze and the asymptotic free electron density $n_0^{(0)}$ may be prescribed. The effective ion charge, screened at large distance, is $Z_\mathrm{eff}\mathrm{e} = (Z - Z_\mathrm{bd})e$, where Z_bd is the number of mobile bound electrons per ion. This must be determined self-consistently [8–10] from the bare charge Ze and the asymptotic free electron density $n_0^{(0)}$.

In the limit of zero electron charge the expression (4.1) for the friction coefficient reduces to that found for the Lorentz-model [7]. The electrical conductivity corresponding to the frequency-dependent friction coefficient in (4.1) is

$$\sigma(\omega) = \frac{n_0^{(0)}e^2}{-i\omega m + \zeta_1(\omega)}. \tag{4.7}$$

The friction coefficient is frequently expressed in terms of the electron–ion collision frequency ν_ei by

$$\nu_\mathrm{ei}(\omega) = \zeta_1(\omega)/m. \tag{4.8}$$

The subscript 1 indicates that only a single scatterer is involved in the calculation of the friction coefficient. In principle, interference effects between two ions may be considered. This would involve a study of the pair contribution in the cluster expansion.

In order to evaluate the single-ion friction coefficient $\zeta_1(\omega)$ given by (4.1) we must solve a linearized Vlasov equation in the presence of the screened ion potential $v_0(r)$, namely

$$-i\omega f_{1\alpha} + \frac{\mathbf{p}}{m}\cdot\frac{\partial f_{1\alpha}}{\partial \mathbf{r}} + \mathbf{F}_0(\mathbf{r})\cdot\frac{\partial f_{1\alpha}}{\partial \mathbf{p}} - e\mathbf{E}_{1\alpha}(\mathbf{r})\cdot\frac{\partial f_0}{\partial \mathbf{p}} = F_{0\alpha}(\mathbf{r})\varphi_0'(r,p) \tag{4.9}$$

with first-order electric field $\mathbf{E}_{1\alpha}(\mathbf{r})$ given by

$$\mathbf{E}_{1\alpha}(\mathbf{r}) = e\frac{\partial}{\partial \mathbf{r}}\int \frac{1}{|\mathbf{r}-\mathbf{r}'|} f_{1\alpha}(\mathbf{r}',\mathbf{p}')\,d\mathbf{r}'\,d\mathbf{p}' \tag{4.10}$$

for each of the three Cartesian components $\alpha = (x,y,z)$. The friction coefficient follows from the solution as

$$\zeta_1(\omega) = -\frac{1}{3}n_\mathrm{i}\iint \mathbf{F}_\mathrm{b}(\mathbf{r})\cdot\mathbf{f}_1(\mathbf{r},\mathbf{p},\omega)\,d\mathbf{r}\,d\mathbf{p}. \tag{4.11}$$

It is worthwhile to consider the exact high-frequency behaviour of the friction coefficient that follows from these expressions. This is given by

$$\zeta_1(\omega) = \frac{1}{3i\omega}n_\mathrm{i}\int \mathbf{F}_\mathrm{b}(\mathbf{r})\cdot\mathbf{F}_0(\mathbf{r})\varphi_0'(r,p)\,d\mathbf{r}\,d\mathbf{p} + O(1/\omega^2). \tag{4.12}$$

https://doi.org/10.1017/S002237780500382X Published online by Cambridge University Press

For an ion with a point nucleus with charge $Z_{\rm p}$e the bare potential $v_{\rm b}(r)$ diverges at short distance as $-Z_{\rm p}{\rm e}^2/r$, and so does the shielded potential $v_0(r)$. Since the potential is attractive, the distribution $\varphi_0(r,p)$ makes the short-distance singularity even worse. For such a potential the short-time coefficient in (4.12) diverges. For an attractive force, the classical model considered here can handle only soft pseudopotentials without point nucleus. The pseudopotential must follow from a separate quantummechanical calculation.

5. Energy-loss theory

The expression for the dynamical friction coefficient derived in the preceding section is closely related to approximate expressions derived for the energy loss of a charged particle moving through an electron gas, in terms of the dielectric function $\epsilon(k,\omega)$ of the uniform plasma. The theory is sometimes known as the dielectric theory. Excellent reviews of energy-loss theory have been presented by Pines and Nozières [2], Calkin and Nicholson [3], and Gerlach and Grosse [11, 12]. Similar approximate results have been derived in the theory of conductivity in the work of Dawson and Oberman [13], Perel' and Eliashberg [14], Ron and Tzoar [15], and Götze and Wölfle [16]. The last three papers are based on quantummechanics. Early attempts to reconcile energy-loss theory with the effect of binary collisions, as described by the Boltzmann equation, have been reviewed by Kihara and Aono [17].

The approximate result of energy-loss theory may be expressed in terms of the friction coefficient as

$$\zeta_1^{(\epsilon)}(\omega) = \frac{2\pi^2 i}{3Z{\rm e}^2\omega}\int k^4|\hat{v}_{\rm b}(k)|^2\left(\frac{1}{\epsilon(k,\omega)}-\frac{1}{\epsilon(k,0)}\right)d\mathbf{k}, \tag{5.1}$$

where $\hat{v}_{\rm b}(k)$ is defined by

$$\hat{v}_{\rm b}(k) = \frac{1}{8\pi^3}\int \exp[-i\mathbf{k}\cdot\mathbf{r}]v_{\rm b}(r)\,d\mathbf{r}. \tag{5.2}$$

In particular, the expression of Dawson and Oberman [13] for a classical plasma with bare potential $v_{\rm b}(r) = -Z{\rm e}^2/r$ reads

$$\zeta_1^{(\epsilon)}(\omega) = \frac{2i}{3\pi}\frac{Z{\rm e}^2}{\omega}\int_0^{k_{\max}}\left(\frac{1}{\epsilon(k,\omega)}-\frac{1}{\epsilon(k,0)}\right)k^2\,dk. \tag{5.3}$$

Here a wavenumber cutoff $k_{\max}$ is required, because of the point singularity in the potential, and $\epsilon(k,\omega)$ is the dielectric function of the uniform electron gas at temperature T.

In order to relate these expressions to (4.11), we first rewrite the latter as an integral over wavevectors by use of Parseval's theorem. This yields

$$\zeta_1(\omega) = -\frac{8\pi^3}{3}n_{\rm i}\iint \hat{\mathbf{F}}^*_{\rm b\mathbf{k}}\cdot\hat{\mathbf{f}}_{\mathbf{k}}(\mathbf{p},\omega)\,d\mathbf{k}\,d\mathbf{p}, \tag{5.4}$$

where $\hat{\mathbf{F}}_{\rm b\mathbf{k}} = -i\mathbf{k}\hat{v}_{\rm b}(k)$ and $\hat{\mathbf{f}}_{\mathbf{k}}(\mathbf{p},\omega)$ is defined as in (5.2). The linearized Vlasov equation (4.9) is approximated by

$$-i\omega f_{1\alpha} + \frac{\mathbf{p}}{m}\cdot\frac{\partial f_{1\alpha}}{\partial\mathbf{r}} - e\mathbf{E}_{1\alpha}(\mathbf{r})\cdot\frac{\partial f_0^{(0)}}{\partial\mathbf{p}} = F_{0\alpha}(\mathbf{r})\varphi_0^{(0)\prime}(p), \tag{5.5}$$

https://doi.org/10.1017/S002237780500382X Published online by Cambridge University Press

where $\varphi_0^{(0)}(p) = \varphi_0(p^2/2m)$ is the asymptotic stationary distribution, and correspondingly $f_0^{(0)}(p) = n_0^{(0)}\varphi_0^{(0)}(p)$. The effect of the shielded force $\mathbf{F}_0(\mathbf{r})$ is omitted on the left-hand side of the equation, and on both sides the distribution $\varphi_0(r,p)$ is approximated by the uniform $\varphi_0^{(0)}(p)$. The dielectric function of the uniform electron gas with distribution $\varphi_0^{(0)}(p)$ is given by [2,3]

$$\epsilon(k,\omega) = 1 + \frac{\omega_{\mathrm{p}0}^2}{k^2}\int \frac{\mathbf{k}\cdot\mathbf{p}}{\omega - \mathbf{k}\cdot\mathbf{p}/m}\varphi_0^{(0)\prime}(p)\,d\mathbf{p}. \tag{5.6}$$

Here

$$\omega_{\mathrm{p}0} = \sqrt{\frac{4\pi n_0^{(0)}e^2}{m}} \tag{5.7}$$

is the plasma frequency. Solving the approximated linearized Vlasov equation (5.5) in a familiar manner by the Fourier transform, one finds for the friction coefficient the approximate expression

$$\zeta_1^{(0)}(\omega) = -\frac{8\pi^3 i}{3}n_{\mathrm{i}}\int \hat{\mathbf{F}}_{\mathrm{b}\mathbf{k}}^{*}\cdot\hat{\mathbf{F}}_{0\mathbf{k}}\frac{\Phi(k,\omega)}{\epsilon(k,\omega)}\,d\mathbf{k} \tag{5.8}$$

with the abbreviation

$$\Phi(k,\omega) = \int \frac{\varphi_0^{(0)\prime}(p)}{\omega - \mathbf{k}\cdot\mathbf{p}/m}\,d\mathbf{p} = \frac{k^2}{m\omega\omega_{\mathrm{p}0}^2}[\epsilon(k,\omega) - \epsilon(k,0)]. \tag{5.9}$$

The energy-loss expression (5.1) is recovered if in (5.8) we approximate the Fourier transform of the shielded force $\mathbf{F}_0(\mathbf{r})$ by

$$\hat{\mathbf{F}}_{0\mathbf{k}}^{(0)} = \hat{\mathbf{F}}_{\mathrm{b}\mathbf{k}}/\epsilon(k,0) \tag{5.10}$$

and use electroneutrality $Zn_{\mathrm{i}} = n_0^{(0)}$. From (5.6) one finds for the zero-frequency value of the dielectric function

$$\epsilon(k,0) = 1 + \frac{\kappa^2}{k^2}, \quad \kappa^2 = -4\pi n_0^{(0)}e^2\int \varphi_0^{(0)\prime}(p)\,d\mathbf{p}. \tag{5.11}$$

For the Maxwell–Boltzmann distribution

$$\varphi_{0\mathrm{MB}}^{(0)}(p) = \left(\frac{\beta}{2\pi m}\right)^{3/2}\exp\left[-\frac{\beta p^2}{2m}\right] \tag{5.12}$$

with $\beta = 1/k_{\mathrm{B}}T$ the inverse screening length κ equals $\sqrt{4\pi n_0^{(0)}e^2/k_{\mathrm{B}}T}$.

Generally, the short-time coefficient A_1 may be defined by

$$\zeta_1(\omega) \approx \frac{A_1}{-i\omega} \quad \text{as } \omega \to \infty. \tag{5.13}$$

From (5.8), (5.9), and (5.11) one finds the approximate value

$$A_1^{(0)} = \frac{8\pi^3}{3Z\mathrm{e}^2}\kappa^2\int_0^\infty \hat{v}_{\mathrm{b}}(k)^{*}\hat{v}_0(k)k^4\,dk. \tag{5.14}$$

Similarly, from (5.1),

$$A_1^{(\epsilon)} = \frac{8\pi^3}{3Z\mathrm{e}^2}\kappa^2\int_0^\infty |\hat{v}_{\mathrm{b}}(k)|^2\frac{k^6}{k^2+\kappa^2}\,dk. \tag{5.15}$$

https://doi.org/10.1017/S002237780500382X Published online by Cambridge University Press

In both (5.14) and (5.15) a wavenumber cutoff may be necessary. It is true that if the quantummechanical Lindhard dielectric function [18] is used the divergence is avoided. If the bare potential has a point singularity $-Z_{\rm p}{\rm e}^2/r$ the friction coefficient then falls off at high frequency [15] in proportion to $\omega^{-3/2}$. A full calculation based on the quantum Vlasov equation must determine the details of the high-frequency behaviour in the presence of quantum effects.

6. Energy-loss theory with pseudopotential

In our explicit calculations we have chosen a particular pseudopotential that has been used in a different context before [19]. The bare pseudopotential in our example has Coulomb behaviour at large distance, but is finite at the origin. As a consequence the high-frequency coefficient in (4.12) is finite. In this section we compare the friction coefficient $\zeta_1^{(\epsilon)}(\omega)$ of energy-loss theory, given by (5.1), with the friction coefficient $\zeta_1^{(0)}(\omega)$ calculated from the uniform plasma approximation, but with the fully screened potential, as given by (5.8). The complete calculation of the friction coefficient $\zeta_1(\omega)$ in Vlasov approximation with the full ion potential, as given by (4.1), is more laborious, and is postponed to the next two sections.

We consider a bare ion potential corresponding to the bare charge density

$$\rho_{\rm b}(r) = \frac{Z{\rm e}}{4\pi}\alpha^2\frac{e^{-\alpha r}}{r} \tag{6.1}$$

with total charge $Z{\rm e}$. The corresponding bare potential is

$$v_{\rm b}(r) = -\frac{Z{\rm e}^2}{r}(1-e^{-\alpha r}). \tag{6.2}$$

At the origin this takes the value $v_{\rm b}(0) = -Z{\rm e}^2\alpha$. The stationary electron distribution is assumed to be given by a Fermi–Dirac distribution at $T = 0$ with Fermi-energy ε_0. Therefore, the asymptotic density $n_0^{(0)}$ is related to the energy by

$$n_0^{(0)} = \frac{8\pi}{3h^3}(2m\varepsilon_0)^{3/2}, \tag{6.3}$$

where $h = 2\pi\hbar$ is Planck's constant. The local stationary electron density is related to the screened potential $\phi_0(r)$ by

$$n_0(r) = \frac{8\pi}{3}\left[\frac{2m}{h^2}(\varepsilon_0 + e\phi_0(r))\right]^{3/2}, \tag{6.4}$$

and by Poisson's equation

$$\nabla^2\phi_0 = 4\pi e\big[n_0(r) - n_0^{(0)}\big] - 4\pi\rho_{\rm b}(r). \tag{6.5}$$

The inverse length α in (6.1) will be determined from the Fermi-energy ε_0 by the exact quantummechanical condition [20]

$$\left.\frac{dn_0}{dr}\right|_{r=0} = -\frac{2Z}{a_0}n_0(0) \tag{6.6}$$

with Bohr radius $a_0 = \hbar^2/me^2$.

In our numerical calculation we choose the particular value $\varepsilon_0 = e^2/2a_0$. In terms of the mean interparticle distance r_0, defined by $(4\pi/3)n_0^{(0)}r_0^3 = 1$, this implies a value $r_{\rm s} = (9\pi/4)^{1/3} = 1.919$ for the dimensionless distance $r_{\rm s} = r_0/a_0$, slightly less than for most metals under normal pressure. For $r_{\rm s}\ll 1$ the system properties

https://doi.org/10.1017/S002237780500382X Published online by Cambridge University Press

are supposed to be well described by the random phase approximation [2], i.e. by energy-loss theory. In atomic units with $e = 1$, $\hbar = 1$, $m = 1$ the electron number density and plasma frequency are

$$n_0^{(0)} = 0.0338, \quad \omega_{\mathrm{p}0} = 0.651. \tag{6.7}$$

In order to find the precise connection between the inverse distance α and the Fermi-energy ε_0 one must solve the Thomas–Fermi equation [10,18] for the screened potential $\phi_0(r)$. In terms of the dimensionless distance $x = \alpha r/\gamma$ with coefficient

$$\gamma = Z^{-1/3} b a_0 \alpha, \quad b = \frac{1}{2}\left(\frac{3\pi}{4}\right)^{2/3} = 0.8853, \tag{6.8}$$

and function $\chi(x)$ defined by

$$\phi_0(r) = \frac{Z\mathrm{e}}{r}\chi(x) \tag{6.9}$$

the equation reads

$$\frac{d^2\chi(x)}{dx} = \frac{1}{\sqrt{x}}\left[[\chi(x) + Cx]^{3/2} - C^{3/2}x^{3/2}\right] - \gamma^2 e^{-\gamma x} \tag{6.10}$$

with coefficient C defined by

$$C = \left(\frac{4\pi b^3 a_0^3 n_0^{(0)}}{Z^2}\right)^{2/3}. \tag{6.11}$$

The Thomas–Fermi equation (6.10) is solved for small x by

$$\chi(x) = d_1 x - \tfrac{1}{2}\gamma^2 x^2 + O(x^3), \tag{6.12}$$

and for large x by

$$\chi(x) \approx \chi_\mu \exp(-\mu x) + \chi_\gamma \exp(-\gamma x) \quad \text{as } x \to \infty \tag{6.13}$$

with coefficients d_1, χ_μ and χ_γ to be determined. The value of μ is found as

$$\mu = [\tfrac{9}{4}C]^{1/4}, \tag{6.14}$$

and the coefficient χ_γ as

$$\chi_\gamma = \left[\frac{3\sqrt{C}}{2\gamma^2} - 1\right]^{-1}. \tag{6.15}$$

The coefficients d_1 and χ_μ are found numerically from the solution. With $\varepsilon_0 = e^2/2a_0$ and $Z = 1$ we find

$$d_1 = 1.318, \quad \chi_\mu = 1.225. \tag{6.16}$$

Hence, we find

$$\begin{aligned} \alpha &= 2.303, \quad \gamma = 2.039, \\ \chi_\gamma &= 1.316, \quad \mu = 0.999. \end{aligned} \tag{6.17}$$

In Fig. 1 we plot the bare ion potential $v_{\mathrm{b}}(r)$ and the screened potential $v_0(r)$ for $Z = 1$ and $\varepsilon_0 = e^2/2a_0$. In Fig. 2 we plot the corresponding Fourier transforms $\hat{v}_{\mathrm{b}}(k)$ and $\hat{v}_0(k)$. The Fourier transform $\hat{v}_{\mathrm{b}}(k)$ is given by

$$\hat{v}_{\mathrm{b}}(k) = -\frac{Z\mathrm{e}^2}{2\pi^2}\frac{\alpha^2}{k^2(k^2+\alpha^2)}. \tag{6.18}$$

https://doi.org/10.1017/S002237780500382X Published online by Cambridge University Press

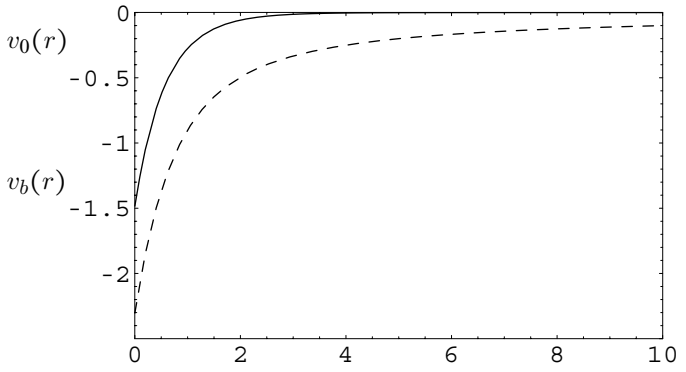


Figure 1. Plot of the bare ion pseudopotential $v_{\rm b}(r)$ (dashed curve), given by (6.2) and (6.17) for $Z = 1$, and the screened ion pseudopotential $v_0(r)$ (full curve) in atomic units for the Thomas–Fermi model, as described in Sec. 6.

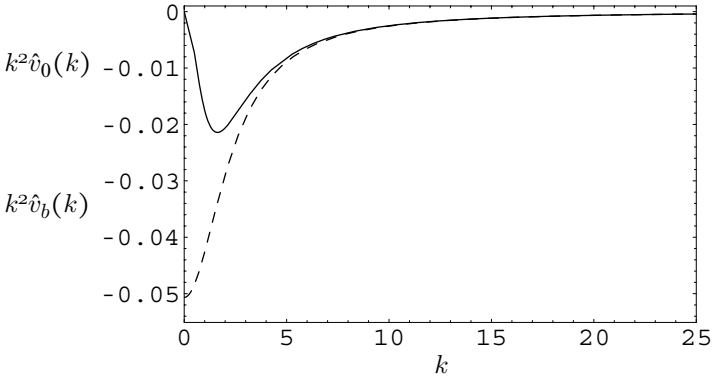


Figure 2. Plot of the Fourier transforms $k^2\hat{v}_{\rm b}(k)$ (dashed curve) and $k^2\hat{v}_0(k)$ (full curve) of the potentials shown in Fig. 1.

The Fourier transform $\hat{v}_0(k)$ of the screened potential is found by numerical transform of the solution of the Thomas–Fermi equation.

The dielectric function for the uniform electron gas with Fermi–Dirac distribution at $T = 0$ is given by [2, 3]

$$\epsilon(k,\omega) = \begin{cases} \epsilon_1(k,\omega), & \left|\dfrac{\omega}{k}\right| > \sqrt{\dfrac{2\varepsilon_0}{m}}, \\ \epsilon_2(k,\omega), & \left|\dfrac{\omega}{k}\right| < \sqrt{\dfrac{2\varepsilon_0}{m}}, \end{cases} \tag{6.19}$$

with

$$\begin{aligned} \epsilon_1(k,\omega) &= 1 + 3\frac{u_{\rm p0}^2}{u_0^2}\left[1 + \frac{u}{2u_0}\log\left(\frac{u-u_0}{u+u_0}\right)\right], \quad |u| > u_0, \\ \epsilon_2(k,\omega) &= 1 + 3\frac{u_{\rm p0}^2}{u_0^2}\left[1 + \frac{u}{2u_0}\log\left(\frac{u_0-u}{u_0+u}\right) + \frac{\pi i}{2}\frac{u}{u_0}\right], \quad |u| < u_0, \end{aligned} \tag{6.20}$$

https://doi.org/10.1017/S002237780500382X Published online by Cambridge University Press

where $u = \omega/k$, $u_0 = \sqrt{2\varepsilon_0/m}$, $u_{\mathrm{p}0} = \omega_{\mathrm{p}0}/k$. In particular, for $\omega = 0$ the dielectric function is real, as in (5.11), with the value

$$\kappa = \sqrt{\frac{3m\omega_{\mathrm{p}0}^2}{2\varepsilon_0}}. \tag{6.21}$$

The numerical value for our example is in atomic units

$$\kappa = 1.128. \tag{6.22}$$

At $\omega = 0$, the function $\Phi(k,\omega)$ defined in (5.9) takes the value

$$\Phi(k,0) = \frac{3\pi i}{2}\frac{m^2}{(2m\varepsilon_0)^{3/2}k}. \tag{6.23}$$

Hence, for the present model the zero-frequency friction coefficient $\zeta_1^{(0)}(0)$ becomes

$$\zeta_1^{(0)}(0) = 16\pi^5\frac{n_{\mathrm{i}}m^2}{(2m\varepsilon_0)^{3/2}}\int_0^\infty \hat{v}_{\mathrm{b}}(k)^*\hat{v}_0(k)\frac{k^5}{k^2+\kappa^2}\,dk \tag{6.24}$$

with numerical value

$$\zeta_1^{(0)}(0) = 0.114. \tag{6.25}$$

The corresponding expression in the dielectric theory is

$$\zeta_1^{(\epsilon)}(0) = 16\pi^5\frac{n_i m^2}{(2m\varepsilon_0)^{3/2}}\int_0^\infty |\hat{v}_{\mathrm{b}}(k)|^2\frac{k^7}{(k^2+\kappa^2)^2}\,dk \tag{6.26}$$

with numerical value

$$\zeta_1^{(\epsilon)}(0) = 0.121. \tag{6.27}$$

The short-time coefficient $A_1^{(0)}$, given by (5.14), takes the value

$$A_1^{(0)} = 0.208. \tag{6.28}$$

The short-time coefficient $A_1^{(\epsilon)}$, given by (5.15), takes the value

$$A_1^{(\epsilon)} = 0.220. \tag{6.29}$$

Hence, with the properly screened potential $v_0(r)$ both the steady-state friction coefficient and the short-time coefficient are somewhat smaller than in the dielectric theory.

From (5.8), by integration over angles one finds

$$\zeta_1^{(0)}(\omega) = -\frac{32\pi^4 i}{3}n_{\mathrm{i}}\int_0^\infty \hat{v}_{\mathrm{b}}(k)^*\hat{v}_0(k)\frac{\Phi(k,\omega)}{\epsilon(k,\omega)}k^4\,dk. \tag{6.30}$$

For positive ω the integration over wavenumbers k can be written as a sum of two parts, corresponding to values less or larger than $\omega/\sqrt{2\varepsilon_0/m}$. For frequencies less than the plasma frequency, the first part is pure imaginary. For frequencies larger than the plasma frequency, the first part yields a real contribution corresponding to emission of plasma waves. For each frequency ω larger than the plasma frequency the real part of the dielectric function has a zero $k_0(\omega)$ corresponding to a propagating plasma wave. In Fig. 3 we plot the real part of the friction coefficient $\Re\zeta_1^{(0)}(\omega)$, as calculated from (6.30) for the model discussed above, as a function of frequency, and compare with $\Re\zeta_1^{(\epsilon)}(\omega)$, as calculated from (5.1).

https://doi.org/10.1017/S002237780500382X Published online by Cambridge University Press

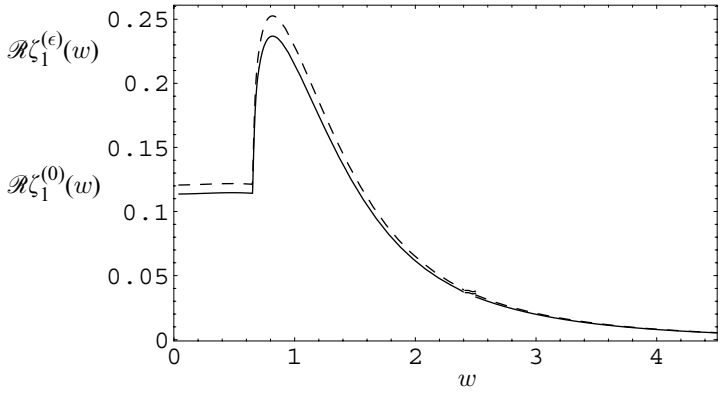


Figure 3. Plot of the real part of the friction coefficient $\Re\zeta_1^{(0)}(\omega)$ as a function of frequency, as given by (6.30) (full curve), and of $\Re\zeta_1^{(\epsilon)}(\omega)$ (dashed curve), as given by (5.1), for the model discussed in Sec. 6.

There is a pronounced resonance starting at the plasma frequency, corresponding to emission of plasma waves. The resonance is also found in a hydrodynamic plasma model [21–23], but in such a model the absorption vanishes for frequency less than the plasma frequency, due to the absence of single-particle excitations.

7. Calculation of friction coefficient

In order to perform a complete calculation of the friction coefficient, taking full account of the ion potential, we must solve the linearized Vlasov equation (4.9). The solution is driven by the inhomogeneous term on the right-hand side of the equation. We solve by making an Ansatz for the solution of similar form to that in the absence of the self-consistent Coulomb field $\mathbf{E}_1(\mathbf{r})$. Thus, we put [7]

$$\mathbf{f}_1(\mathbf{r},\mathbf{p}) = \mathbf{g}(r,p,\xi)\varphi_0'(r,p), \tag{7.1}$$

where $\xi = \hat{\mathbf{r}}\cdot\hat{\mathbf{p}}$, and assume that $\mathbf{g}(r,p,\xi)$ has the form

$$\mathbf{g}(r,p,\xi) = \hat{g}(r,p,\xi)\mathbf{r} + \hat{h}(r,p,\xi)\mathbf{p}. \tag{7.2}$$

Then the fourth term on the left-hand side of (4.9) takes the form

$$e\mathbf{E}_{1\alpha}(\mathbf{r})\cdot\frac{\partial f_0}{\partial\mathbf{p}} = e^2\varphi_0'\frac{\mathbf{p}}{m}\cdot\frac{\partial}{\partial\mathbf{r}}\int\frac{f_0'(r',p')}{|\mathbf{r}-\mathbf{r}'|}[\hat{g}(r',p',\xi')r_\alpha' + \hat{h}(r',p',\xi')p_\alpha']\,d\mathbf{r}'\,d\mathbf{p}'. \tag{7.3}$$

By symmetry this becomes

$$e\mathbf{E}_{1\alpha}(\mathbf{r})\cdot\frac{\partial f_0}{\partial\mathbf{p}} = \varphi_0'\frac{\mathbf{p}}{m}\cdot\frac{\partial}{\partial\mathbf{r}}\hat{\mathscr{T}}(r)r_\alpha \tag{7.4}$$

with $\hat{\mathscr{T}}(r)$ determined by the six-dimensional integral. We may define characteristics in (r,p,ξ)-space corresponding to the motion $(\mathbf{r}(t),\mathbf{p}(t))$ determined by the Hamiltonian $H_0(r,p)$ by the equations [7]

$$\begin{aligned}\frac{dr}{ds} &= \frac{1}{m}\xi p, \quad \frac{dp}{ds} = \xi F_0,\\ \frac{d\xi}{ds} &= (1-\xi^2)\left(\frac{p}{mr}+\frac{F_0}{p}\right),\end{aligned} \tag{7.5}$$

https://doi.org/10.1017/S002237780500382X Published online by Cambridge University Press

with scalar parameter s along the characteristics. Hence, for functions defined in (r, p, ξ)-space we have

$$\frac{d}{ds} = \frac{1}{m}\xi p\frac{\partial}{\partial r} + \xi F_0\frac{\partial}{\partial p} + (1-\xi^2)\left(\frac{p}{mr} + \frac{F_0}{p}\right)\frac{\partial}{\partial \xi}, \tag{7.6}$$

and the expression on the right-hand side of (7.4) becomes

$$\frac{\mathbf{p}}{m}\cdot\frac{\partial}{\partial \mathbf{r}}\hat{\mathscr{T}}(r)\mathbf{r} = \mathbf{r}\frac{d\hat{\mathscr{T}}}{ds} + \frac{\mathbf{p}}{m}\hat{\mathscr{T}}. \tag{7.7}$$

This shows that the Ansatz (7.2) is effective. One finds that the linearized Vlasov equation (4.9) leads to two coupled equations for the two scalar functions $\hat{g}(r, p, \xi)$ and $\hat{h}(r, p, \xi)$,

$$\begin{aligned} -i\omega\hat{g} + \frac{d\hat{g}}{ds} + \frac{F_0}{r}\hat{h} - \frac{d\hat{\mathscr{T}}}{ds} &= \frac{F_0}{r}, \\ -i\omega\hat{h} + \frac{d\hat{h}}{ds} + \frac{1}{m}\hat{g} - \frac{1}{m}\hat{\mathscr{T}} &= 0, \end{aligned} \tag{7.8}$$

where $\hat{\mathscr{T}}(r)$ is linear in the two functions $\hat{g}$ and $\hat{h}$. In order to find the expression for $\hat{\mathscr{T}}(r)$ we must perform the six-dimensional integral on the right-hand side of (7.3).

The six-dimensional integral can be reduced to a three-dimensional integral over the variables r', p', ξ'. The remaining integration is over the azimuthal angle η' of the vector $\mathbf{p}'$ with respect to the vector $\mathbf{r}'$ and the polar angles θ', φ' of the vector $\mathbf{r}'$ with respect to the fixed vector $\mathbf{r}$. The integration over these angles can be performed with the result [24]

$$\int \frac{\mathbf{r}'}{|\mathbf{r}-\mathbf{r}'|}\sin\theta'\, d\theta'\, d\varphi'\, d\eta' = \frac{8\pi^2}{3r'}\Theta\left(\frac{r'}{r}\right)\mathbf{r}, \tag{7.9}$$

with

$$\Theta(u) = \begin{cases} u^3, & u < 1, \\ 1, & u > 1. \end{cases} \tag{7.10}$$

Similarly

$$\int \frac{\mathbf{p}'}{|\mathbf{r}-\mathbf{r}'|}\sin\theta'\, d\theta'\, d\varphi'\, d\eta' = \frac{8\pi^2 p'\xi'}{3r'^2}\Theta\left(\frac{r'}{r}\right)\mathbf{r}. \tag{7.11}$$

Hence, for the function $\hat{\mathscr{T}}(r)$ we find

$$\begin{aligned} \hat{\mathscr{T}}(r) = \frac{8\pi^2 e^2}{3}\int_0^\infty\int_0^\infty\int_{-1}^1 f_0'(r', p')\Theta\left(\frac{r'}{r}\right) \\ \times\left[\frac{1}{r'}\hat{g}(r', p', \xi') + \frac{p'\xi'}{r'^2}\hat{h}(r', p', \xi')\right] r'^2 p'^2\, dr'\, dp'\, d\xi'. \end{aligned} \tag{7.12}$$

We can regard the functions $\hat{g}(r, p, \xi, \omega)$ and $\hat{h}(r, p, \xi, \omega)$ as Laplace-transforms of time-dependent functions $g(r, p, \xi, t)$ and $h(r, p, \xi, t)$ defined as

$$\hat{g}(r, p, \xi, \omega) = \int_0^\infty \exp(i\omega t) g(r, p, \xi, t)\, dt, \tag{7.13}$$

https://doi.org/10.1017/S002237780500382X Published online by Cambridge University Press

and similarly for $\hat{h}(r,p,\xi,\omega)$. With this definition, (7.8) can be regarded as the Laplace-transform of the pair of integro-differential equations

$$\begin{aligned}\frac{\partial g}{\partial t}+\frac{\partial g}{\partial s}+\frac{F_0}{r}h&=\frac{\partial \mathscr{T}}{\partial s},\\ \frac{\partial h}{\partial t}+\frac{\partial h}{\partial s}+\frac{1}{m}g&=\frac{1}{m}\mathscr{T},\end{aligned}\tag{7.14}$$

to be solved with initial conditions

$$g(r,p,\xi,0)=\frac{F_0(r)}{r},\quad h(r,p,\xi,0)=0.\tag{7.15}$$

Here $\mathscr{T}$ is defined as in (7.12), but with $\hat{g}(\omega)$ and $\hat{h}(\omega)$ replaced by $g(t)$ and $h(t)$.

By substitution of (7.1) and (7.2), the friction coefficient in (4.11) may be expressed as

$$\zeta_1(\omega)=-\frac{8\pi^2}{3}n_i\int\varphi_0'(r,p)F_{\rm b}(r)[r\hat{g}(r,p,\xi)+\xi p\hat{h}(r,p,\xi)]r^2p^2\,dr\,dp\,d\xi.\tag{7.16}$$

The characteristics defined by (7.5) are the intersections of the surfaces in (r,p,ξ)-space of constant $H_0(r,p)=\varepsilon$ and constant $L(r,p,\xi)=\lambda$, where

$$L(r,p,\xi)=|\mathbf{r}\times\mathbf{p}|=rp\sqrt{1-\xi^2}\tag{7.17}$$

is the angular momentum. The three-dimensional integral in (7.16) is performed conveniently by transformation to the variables $(\varepsilon,\lambda^2,s)$. From the Jacobian of the transformation one finds for the new volume element [7, 24]

$$d\varepsilon\,d\lambda^2\,ds=2r^2p^2\,dr\,dp\,d\xi.\tag{7.18}$$

The friction coefficient becomes

$$\zeta_1(\omega)=-\frac{4\pi^2}{3}n_{\rm i}\int\varphi_0'(\varepsilon)F_{\rm b}(r)[r\hat{g}+\xi p\hat{h}]\,d\varepsilon\,d\lambda^2\,ds.\tag{7.19}$$

This can be written

$$\zeta_1(\omega)=-\frac{4\pi^2}{3}n_{\rm i}\int\varphi_0'(\varepsilon)\hat{C}_+(\omega;\varepsilon,\lambda)\,d\varepsilon\,d\lambda^2\tag{7.20}$$

with transform

$$\hat{C}_+(\omega;\varepsilon,\lambda)=\int_0^\infty e^{i\omega t}C(t;\varepsilon,\lambda)\,dt\tag{7.21}$$

of the force correlation function

$$C(t;\varepsilon,\lambda)=\int_{-\infty}^{\infty}F_{\rm b}(r)F_0(r,t)\,ds.\tag{7.22}$$

Here the time-dependent screened force $F_0(r,t)$ is given by

$$F_0(r,t)=rg(s,t)+\xi ph(s,t),\tag{7.23}$$

where $g(s,t),h(s,t)$ is the solution of (7.14) with initial conditions (7.15). Along each characteristic the variables (r,p,ξ) are functions $(r(s;\varepsilon,\lambda),p(s;\varepsilon,\lambda),\xi(s;\varepsilon,\lambda))$ of the orbit parameter s, chosen such that $s=0$ for $\xi=0$. The distance function $r(s;\varepsilon,\lambda)$ is found as solution of the first-order differential equation

$$\frac{dr}{ds}=\sqrt{\frac{2}{m}}\left[\varepsilon-v_0(r)-\frac{\lambda^2}{2mr^2}\right]^{1/2}\tag{7.24}$$

https://doi.org/10.1017/S002237780500382X Published online by Cambridge University Press

with symmetry $r(s) = r(-s)$. Hence, the momentum $p(s;\varepsilon,\lambda)$ is found as

$$p(s;\varepsilon,\lambda) = \sqrt{2m[\varepsilon - v_0(r(s;\varepsilon,\lambda))]}. \tag{7.25}$$

Finally $\xi(s;\varepsilon,\lambda)$ is found as

$$\xi(s;\varepsilon,\lambda) = \pm\sqrt{1 - \frac{\lambda^2}{r(s;\varepsilon,\lambda)^2 p(s;\varepsilon,\lambda)^2}} \tag{7.26}$$

with symmetry $\xi(s) = -\xi(-s)$.

The solution of (7.14) is calculated separately for each characteristic, at first treating the right-hand side as a known inhomogeneous term. Subsequently, the right-hand side is calculated from an integral over characteristics, and the equation is made self-consistent. In our numerical calculation this is performed in small timesteps, readjusting the inhomogeneous term after each timestep. Thus assuming the solution $(g(s,t), h(s,t))$ to be known at time t for characteristic (ε,λ), we write for the solution at time $t+\Delta t$

$$\begin{aligned} g(s,t+\Delta t) &= [-\psi_1'(s)\psi_2(s-\Delta t) + \psi_2'(s)\psi_1(s-\Delta t)]g(s-\Delta t,t) \\ &\quad - m[\psi_1'(s)\psi_2'(s-\Delta t) + \psi_2'(s)\psi_1'(s-\Delta t)]h(s-\Delta t,t) + \frac{\partial \mathscr{T}}{\partial s}\Delta t, \\ h(s,t+\Delta t) &= \frac{1}{m}[\psi_1(s)\psi_2(s-\Delta t) - \psi_2(s)\psi_1(s-\Delta t)]g(s-\Delta t,t) \\ &\quad + [\psi_1(s)\psi_2'(s-\Delta t) - \psi_2(s)\psi_1'(s-\Delta t)]h(s-\Delta t,t) + \frac{1}{m}\mathscr{T}\Delta t, \end{aligned} \tag{7.27}$$

where $\psi_1(s), \psi_2(s)$ are solutions of the equation

$$m\frac{d^2\psi}{ds^2} - \frac{F_0(r(s))}{r(s)}\psi = 0 \tag{7.28}$$

satisfying the conditions

$$\begin{aligned} \psi_1(0) &= 1, \quad \psi_1'(0) = 0, \\ \psi_2(0) &= 0, \quad \psi_2'(0) = 1. \end{aligned} \tag{7.29}$$

The first two terms on the right-hand side of (7.27) provide the solution of the homogeneous equations, valid for any length of the timestep. The last terms provide an approximation to the particular solution of the inhomogeneous equations, and are only valid to first order in the timestep Δt. In terms of the variables (ε,λ,s) the function $\mathscr{T}(r,t)$ reads [24]

$$\begin{aligned} \mathscr{T}(\varepsilon,\lambda,s,t) &= \frac{4\pi^2 e^2}{3}\int_{\varepsilon_{\min}}^{\infty}\int_0^{\infty}\int_{-\infty}^{\infty} f_0'(\varepsilon')\frac{1}{r(s';\varepsilon',\lambda')}\Theta\left(\frac{r(s';\varepsilon',\lambda')}{r(s;\varepsilon,\lambda)}\right) \\ &\quad \times\left[g(s',t;\varepsilon',\lambda') + \frac{p(s';\varepsilon',\lambda')\xi(s';\varepsilon',\lambda')}{r(s';\varepsilon',\lambda')}h(s',t;\varepsilon',\lambda')\right] d\varepsilon'\, d\lambda'^2\, ds'. \end{aligned} \tag{7.30}$$

The function $\mathscr{T}(t+\Delta t)$ is calculated from the solution (7.27), and the procedure is repeated for the next timestep. The initial conditions are $g(s,0) = F_0(r(s))/r(s)$, $h(s,0) = 0$, and the function $\mathscr{T}(r,0)$ is calculated from these values by integration over $(\varepsilon',\lambda',s')$. At each timestep the force correlation function $C(t;\varepsilon,\lambda)$ is calculated from (7.22) and integrated over (ε,λ). After a time interval of sufficient length the

https://doi.org/10.1017/S002237780500382X Published online by Cambridge University Press

friction coefficient $\zeta_1(\omega)$ is evaluated by one-sided Fourier-transform with respect to time.

8. Numerical results

In our numerical work we have considered the example discussed already in Sec. 6 with a particular choice of ion potential and a Fermi–Dirac distribution at $T = 0$ with Fermi-energy ε_0. Thus, the stationary distribution is

$$\varphi_0(\varepsilon) = \frac{3}{4\pi}(2m\varepsilon_0)^{-3/2}\theta(\varepsilon_0 - \varepsilon), \tag{8.1}$$

where $\theta(x)$ is the Heaviside step function. We consider the case $\varepsilon_0 = 0.5$ in atomic units. The bare ion potential $v_{\mathrm{b}}(r)$ and the screened ion potential $v_0(r)$ have been discussed in Sec. 6.

The initial value of the force correlation function $C(t;\varepsilon)$, defined by

$$C(t;\varepsilon) = \int_0^\infty C(t;\varepsilon,\lambda)\, d\lambda^2, \tag{8.2}$$

may be evaluated by use of (7.22) as

$$C(0;\varepsilon) = \int_0^\infty \int_{-\infty}^\infty F_{\mathrm{b}}(r(s;\varepsilon,\lambda))F_0(r(s;\varepsilon,\lambda))\, d\lambda^2\, ds. \tag{8.3}$$

We find in our example

$$C(0;\varepsilon_0) = 2.604. \tag{8.4}$$

This corresponds to the value

$$A_1 = 0.276 \tag{8.5}$$

for the short-time coefficient, as determined by (5.13) and (7.20). This is to be compared with the approximate values given by (6.28) and (6.29). At high frequency the friction coefficient is larger in absolute value than predicted by energy-loss theory.

In our example the numerical calculation of the time-correlation function is simplified, since the derivative of the stationary distribution $\varphi_0'(\varepsilon)$ is proportional to a delta-function. Nonetheless, the calculation is time consuming, because at each timestep the functions $g(s,t;\varepsilon,\lambda)$ and $h(s,t;\varepsilon,\lambda)$ must be evaluated for a large number of discrete angular momenta λ. In order to speed up the numerical calculation we do a preliminary calculation of the orbits $r(s;\varepsilon,\lambda)$ and represent the deviation from the free motion for each orbit as a sum of two exponentials. The latter are calculated by the method of Padé approximants [25]. This provides an accurate analytic representation of the orbits.

In Fig. 4 we plot the time-correlation function $C(t;\varepsilon_0)$, as calculated by the numerical procedure indicated in Sec. 7. In Fig. 5 we plot the real part of the friction coefficient $\Re\zeta_1(\omega)$ as a function of frequency and compare with the approximate $\Re\zeta_1^{(0)}(\omega)$, as calculated in Sec. 6. Again there is a pronounced resonance at the plasma frequency, but the discontinuity in slope of the approximate theory is eliminated. The value of the zero-frequency friction coefficient is

$$\zeta_1(0) = 0.081. \tag{8.6}$$

This is to be compared with the approximate values given in (6.25) and (6.27). The steady-state friction coefficient is smaller than predicted by energy-loss theory.

https://doi.org/10.1017/S002237780500382X Published online by Cambridge University Press

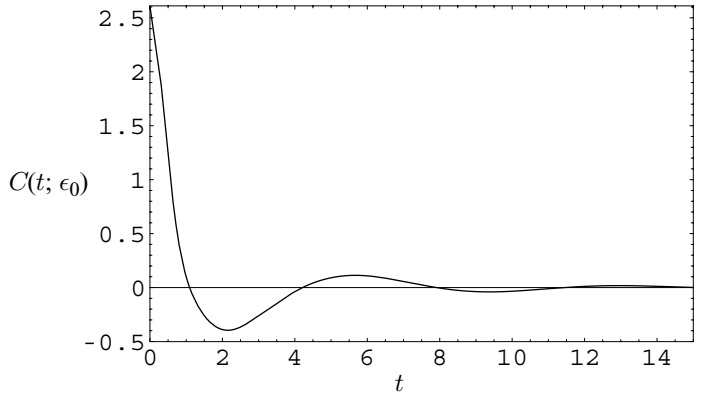


Figure 4. Plot of the time-correlation function $C(t;\varepsilon_0)$ for the model discussed in Sec. 6.

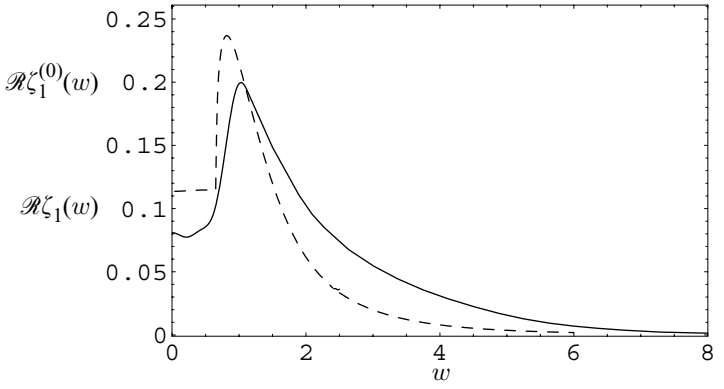


Figure 5. Plot of the real part of the friction coefficient $\Re\zeta_1(\omega)$ as a function of frequency, as given by (4.1) and calculated for the model discussed in Sec. 6 (full curve), compared with $\Re\zeta_1^{(0)}(\omega)$ of energy-loss theory, as given by (6.30) (dashed curve).

9. Discussion

We have shown in the framework of the Lorentz–Vlasov model of a classical plasma that the interaction of a selected ion with the mobile electrons can be fully taken into account. The dynamical friction coefficient calculated in linear response theory differs significantly from that found from dielectric or energy-loss theory, at least for the chosen example. In order to avoid divergence difficulties of the classical theory, and associated arbitrary cutoffs, we have used a smooth ion pseudopotential without point nucleus. It would be of interest to extend the calculation to quantummechanics, where there would be no divergence difficulties. So far, such calculations have been performed in the framework of energy-loss theory [15], with use of Lindhard's dielectric function. A random phase approximation to the total electronic polarizability of a dense partially ionized plasma has been studied by Blenski and Cichocki [26, 27]. A full quantummechanical calculation of the single-ion friction coefficient, along the lines followed here for the classical case, would be very interesting.

Silin [28] and Decker et al. [29] have extended the dielectric theory to the case of nonlinear response. The quantummechanical version of the nonlinear dielectric

https://doi.org/10.1017/S002237780500382X Published online by Cambridge University Press

theory has been discussed by Kull and Plagne [30]. They showed that the use of Lindhard's dielectric function leads to a relatively simple explanation of observed nonlinear photoabsorption phenomena. Time-dependent strong field effects have also been studied in terms of a ballistic model [31].

Relativistic effects in the theory of inverse bremsstrahlung have been discussed by Schlessinger and Wright [32]. A formally exact quantummechanical kinetic theory of plasmas has been elaborated by Kremp et al. [33,34]. It would be desirable to extend the theory presented here to nonlinear response and relativity, both in classical and quantum mechanics, and to compare with the exact kinetic theory.

References

[1] Spitzer, L. Jr. 1962 *Physics of Fully Ionized Gases*. New York: Interscience, p. 127.
[2] Pines, D. and Nozières, P. 1966 *The Theory of Quantum Liquids*. New York: Benjamin.
[3] Calkin, M. G. and Nicholson, P. J. 1967 *Rev. Mod. Phys.* **39**, 361.
[4] Cichocki, B., Felderhof, B. U. and Hinsen, K. 1989 *Phys. Rev.* A **39**, 5350.
[5] Huberman, M. and Chester, G. V. 1975 *Adv. Phys.* **24**, 489.
[6] Kubo, R., Toda, M. and Hashitsume, N. 1991 *Statistical Physics II*. Berlin: Springer.
[7] Felderhof, B. U. 1998 *J. Stat. Phys.* **93**, 307.
[8] Rozsnyai, B. F. 1991 *Phys. Rev.* A **43**, 3035.
[9] Dharma-wardana, M. W. C. and Perrot, F. 1992 *Phys. Rev.* A **45**, 5883.
[10] Ishikawa, K., Felderhof, B. U., Blenski, T. and Cichocki, B. 1998 *J. Plasma Phys.* **60**, 787.
[11] Gerlach, E. and Grosse, P. 1977 *Adv. Solid State Phys.* **17**, 157.
[12] Gerlach, E. 1986 *J. Phys.* C **19**, 4585.
[13] Dawson, J. and Oberman, C. 1962 *Phys. Fluids* **5**, 517.
[14] Perel', V. I. and Eliashberg, G. M. 1962 *Sov. Phys.–JETP* **14**, 633.
[15] Ron, A. and Tzoar, N. 1963 *Phys. Rev.* **131**, 12.
[16] Götze, W. and Wölfle, P. 1972 *Phys. Rev.* B **6**, 1226.
[17] Kihara, T. and Aono, O. 1971 *Kinetic Equations* (ed. R. Liboff and N. Rostoker). New York: Gordon and Breach.
[18] Ashcroft, N. W. and Mermin, N. D. 1976 *Solid State Physics*. New York: Holt, Rinehart and Winston.
[19] Ishikawa, K. and Felderhof, B. U. 1998 *Physica* A **253**, 541.
[20] Roothaan, C. C. J. and Weiss, A. W. 1973 *Rev. Mod. Phys.* **45**, 333.
[21] Felderhof, B. U., Blenski, T. and Cichocki, B. 1995 *Physica* A **217**, 175.
[22] Felderhof, B. U., Blenski, T. and Cichocki, B. 1995 *Physica* A **217**, 196.
[23] Ishikawa, K. and Felderhof, B. U. 1998 *Physica* A **250**, 506.
[24] Thin Le, 1999 *Diploma Thesis*, RWTH Aachen.
[25] Cichocki, B. and Felderhof, B. U. 1994 *Physica* A **211**, 165.
[26] Blenski, T. and Cichocki, B. 1992 *Laser Particle Beams* **10**, 299.
[27] Blenski, T. and Cichocki, B. 1994 *Journal of Quantitative Spectroscopy and Radiactive Transfer* **51**, 49.
[28] Silin, V. P. 1965 *Sov. Phys.–JETP* **20**, 1510.
[29] Decker, C. D., Mori, W. B., Dawson, J. M. and Katsouleas, T. 1994 *Phys. Plasmas* **1**, 4043.
[30] Kull, H.-J. and Plagne, L. 2001 *Phys. Plasmas* **8**, 5244.
[31] Mulser, P., Cornolti, F., Bésuelle, E. and Schneider, R. 2000 *Phys. Rev.* E **63**, 016406.
[32] Schlessinger, L. and Wright, J. 1979 *Phys. Rev.* A **20**, 1934.
[33] Kremp, D., Bornath, Th., Bonitz, M. and Schlanges, M. 1999 *Phys. Rev.* E **60**, 4725.
[34] Bornath, Th., Schlanges, M., Hilse, P. and Kremp, D. 2001 *Phys. Rev.* E **64**, 026414.

https://doi.org/10.1017/S002237780500382X Published online by Cambridge University Press